PhD Forum Abstract: When Do Intelligent Metasurfaces Improve Performance in Cellular Networks?

Julian Santos
Orange Labs and Inria
Paris, France
julian.santos@orange.com

Jean-Marc Kelif
Orange Labs
Paris, France
jeanmarc.kelif@orange.com

***Abstract*—Wireless networks have long treated propagation as a condition to adapt to rather than something to control. Intelligent metasurfaces change that view by making part of the radio environment programmable. However, many reported gains rely on idealized link-level assumptions that may not hold in realistic cellular operation. This dissertation develops a tractable analysis to answer the following question: when do intelligent metasurfaces improve performance in cellular networks? The framework combines stochastic-geometry models of irregular deployments with physically motivated models for reflected-link degradation, including bounded phase errors, spatial correlation across the metasurface aperture, channel dynamics, finite control resolution, and urban-micro propagation. The analysis distinguishes between a beamforming-dominant regime and a diffuse regime. In the first case, reflected contributions add constructively and the useful reflected power can scale quadratically with the number of elements. In the second case, the reflected field is mainly diffuse and the average reflected power grows only linearly. Embedding this degradation into a cellular model shows under which conditions metasurfaces strengthen and stabilize the useful signal, under which conditions the improvement is limited, and how reflected energy contributes to useful signal and interference.**

***Index Terms*—Intelligent metasurfaces, reconfigurable intelligent surfaces, stochastic geometry, cellular networks.**

I. Introduction and Scope

Intelligent metasurfaces, also called reconfigurable intelligent surfaces (RIS), aim to make part of the radio environment programmable [1]–[4]. Their reported gains are often derived under favorable assumptions: accurate channel knowledge, stable phase control, and nearly ideal reflection. These assumptions are fragile in cellular operation. The reflected path is two-hop. The surface is not ideal. The effective aperture depends on geometry. Control quality degrades under mobility and delay.

A metasurface is a compelling solution for cellular networks only if three conditions hold. First, the serving reflected link must be strong enough to produce a useful signal gain. Second, this gain must remain meaningful at network level, despite interference, spatial randomness, and signal fluctuations. Third, the overall benefit must remain positive after accounting for signaling overhead, hardware losses, deployment constraints, and comparison with competing solutions such as repeaters or denser infrastructure. This document addresses the first two conditions. It does not yet resolve the third.

ISBN 978-3-903176-82-9 © 2026 IFIP

The literature can be grouped into three main lines: network-level studies of smart radio environments and cellular performance [1]–[7], link-level analyses of passive beamforming [8], and physically grounded propagation models for reconfigurable surfaces [9]–[13]. What remains missing is a study that carries reflected-link degradation to the cellular level. This document addresses that gap.

The analysis focuses on factors that act directly on the reflected signal: bounded phase mismatch, spatial correlation, channel aging, estimation quality, phase quantization, and propagation geometry. These factors determine whether the serving reflected link remains coherent enough to yield a meaningful network-level gain. If this condition is not met, further implementation and deployment constraints can only reinforce that conclusion. Beam management, protocol signaling, deployment cost, insertion loss, calibration drift, grating lobes, near-field effects, interoperability, and regulation are therefore left aside. These factors may further reduce the gain, shift the regime boundary, or narrow the operating range. The present work should thus be read as a first-order viability analysis rather than a deployment verdict.

This scope is consistent with recent deployment-oriented discussions [14]. Network-controlled repeaters (NCRs) and integrated access and backhaul (IAB) pursue related coverage goals through more established active mechanisms. Metasurfaces instead act through reconfiguration of the propagation environment, and their benefit depends strongly on reflection efficiency, geometry, control quality, and overhead. 3GPP Release-18 and Release-19 did not continue metasurfaces as a study item, whereas 3GPP has concrete work on NCRs and mobile IAB. In parallel, ITU-R identifies metasurfaces as a potential IMT-2030 technology, and ITU-T has an active work item [15]–[19].

Figure 1 shows the two deployment baselines used in this work. The left panel is a Poisson deployment of base stations. The right panel is a density-matched hexagonal deployment.

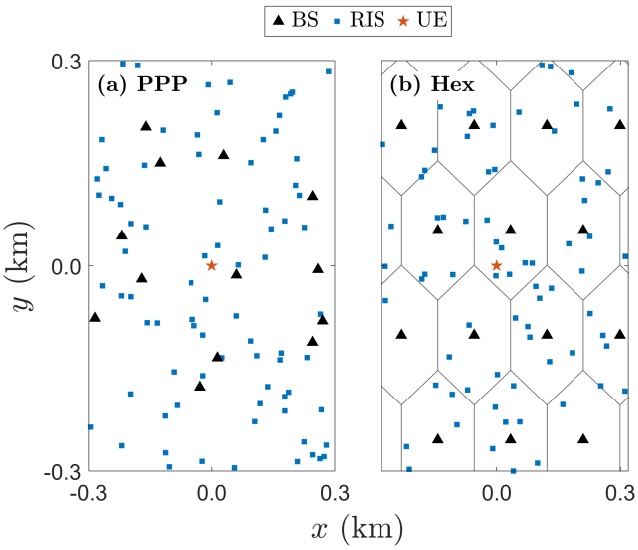

Fig. 1. Deployment baselines used in the analysis. (a) Poisson base-station layout. (b) density-matched hexagonal layout. RIS locations are modeled by a Poisson process in both cases.

The base-station density corresponds to the average density in Paris, France. The Poisson model captures macroscopic irregularity and preserves its effect on received signal quality and interference [20]. The hexagonal model is retained as a regular reference for planned deployments. Using both models helps separate deployment-geometry effects from metasurface-model effects. Metasurfaces are deployed according to a Poisson distribution.

The document makes three contributions. First, it characterizes the transition between beamforming-dominant and diffuse reflected operation under realistic reflected-link degradation. Second, it introduces a compact link model that carries this transition into a tractable cellular model and separates useful reflected energy from metasurface-induced interference. Third, it links the resulting useful-link statistics to deployment-oriented metrics and interprets the results through operating-regime maps rather than idealized reflected-power gains alone.

II. Methodology

This document studies the downlink of a metasurface-assisted cellular network through stochastic geometry. Base stations, users, and metasurfaces are modeled as homogeneous Poisson point processes on $\mathbb{R}^2$, with densities λ_{BS}, λ_{U}, and λ_{M}. The analysis is performed from the viewpoint of the representative user at the origin, served by its nearest base station x_0. Each base station controls metasurfaces only inside a disk of radius R_A.

Two analytical choices are made explicit. First, the metasurfaces over the network are approximated by a Poisson field. Second, conditioned on the serving distance, the useful received power is approximated by a moment-matched Gamma law. These are tractable approximations, not exact physical laws. They preserve the dominant geometry, interference, and fluctuation structure while keeping the framework analyzable.

Large-scale attenuation is written as $\ell(r;H) = (r^2 + H^2)^{-\alpha/2}$ for $\alpha > 2$, where r is the horizontal distance and H is the effective height difference. Specific cases are denoted by $\ell_{\mathrm{BU}}(r) = \ell(r;H_{\mathrm{BU}})$, $\ell_{\mathrm{BM}}(r) = \ell(r;H_{\mathrm{BM}})$, and $\ell_{\mathrm{MU}}(r) = \ell(r;H_{\mathrm{MU}})$. For numerical evaluation, these links are instantiated with the 3GPP TR 38.901 UMi-LOS model.

The central distinction is between a beamforming-dominant regime and a diffuse regime. For a single metasurface, when the residual phase mismatch remains bounded, the received field satisfies

$$\cos(\varepsilon_{\max})\,\bar{a} \le \liminf_{n\to\infty} \frac{|y|}{n} \le \limsup_{n\to\infty} \frac{|y|}{n} \le \bar{a}, \tag{1}$$

so that $|y| = \Theta(n)$ and $|y|^2 = \Theta(n^2)$. Here, y is the received field, n is the number of reflecting elements, $\varepsilon_{\max}$ is the maximum residual phase error, and $\bar{a}$ is the asymptotic average cascaded amplitude per element. In contrast, when the reflected field is diffuse, the average received power satisfies

$$\lim_{n\to\infty} \frac{1}{n}\,\mathbb{E}[|y|^2] = \sum_{u\in\mathbb{Z}^2} R(u), \tag{2}$$

which implies $\mathbb{E}[|y|^2] = O(n)$, where $R(u) = \mathbb{E}[X_0 X_u^*]$ is the covariance at spatial offset u, and X_u is the contribution of the reflecting element at u. If the inter-element spacing remains on the order of $\lambda/2$, then n is proportional to physical aperture area. Under this condition, beamforming-dominant reflected power is quadratic in area, whereas diffuse reflected power is linear in area.

To carry these two behaviors into the network model, the serving reflected contribution is summarized by an effective quality factor $\rho \in [0,1]$. It captures channel aging, imperfect channel estimation, and finite phase resolution, which have each been studied in the literature [12], [13]. A convenient first-order representation is

$$\rho \approx \rho_{\mathrm{age}}\rho_{\mathrm{CSI}}\rho_q \approx |J_0(2\pi f_D \Delta t)|^2 \cdot \frac{\vartheta_t^2 \xi\gamma}{1+\xi\gamma} \cdot \mathrm{sinc}^2\!\left(\frac{\pi}{2^i}\right), \tag{3}$$

where f_D is the Doppler frequency, Δt is the control delay, γ is the pilot SNR, i is the number of metasurface control bits, and ϑ_t, ξ are effective estimation parameters. The product form is an analytical separation of impairments, not an exact independence statement. It defines a compact operating parameter. Its accuracy should be checked by sensitivity analysis or simulation when several impairments are simultaneously strong.

The serving reflected gain contributed by a metasurface at z is modeled as

$$\widetilde{G}_z^{(x_0\to 0)} = \Gamma^2 \zeta_b \eta \big[\rho n^2 + (1-\rho)n\big]\, \ell_{\mathrm{BM}}\big(\|z - x_0\|\big)\, \ell_{\mathrm{MU}}\big(\|z\|\big), \tag{4}$$

where $\Gamma \in [0,1]$ is the reflection efficiency, $\zeta_b \in [0,1]$ is a residual implementation-loss factor not already absorbed into ρ, and $\eta \in [0,1]$ is a projected-aperture factor.

Let $R_0 = \|x_0\|$ be the serving distance and let $\Phi_M^{(x)}$ denote the metasurfaces associated with base station x. All base stations transmit with power P_{tx}, s_x denotes the unit-power symbol sent by base station x, and $w \sim \mathcal{CN}(0, \sigma^2)$ is the additive noise. The direct-link fading coefficients are h_{x_0} for the serving base station and h_x for interfering base stations. The terms $v_z^{(x_0 \to 0)}$ and $v_{z,\mathrm{int}}^{(x \to 0)}$ denote the metasurface-assisted contributions from the serving and interfering links, respectively. Conditioned on the geometry, the received baseband signal is

$$\begin{aligned} y = \sqrt{P_{\mathrm{tx}}} \left(h_{x_0} \ell_{\mathrm{BU}}(R_0)^{1/2} + \sum_{z \in \Phi_M^{(x_0)}} v_z^{(x_0 \to 0)} \right) s_{x_0} \\ + \sum_{x \in \Phi_{\mathrm{BS}} \setminus \{x_0\}} \sqrt{P_{\mathrm{tx}}}\, h_x \ell_{\mathrm{BU}}(\|x\|)^{1/2} s_x \\ + \sum_{x \in \Phi_{\mathrm{BS}} \setminus \{x_0\}} \sum_{z \in \Phi_M^{(x)}} \sqrt{P_{\mathrm{tx}}}\, v_{z,\mathrm{int}}^{(x \to 0)} s_x + w, \end{aligned} \tag{5}$$

where the first line is the useful signal, the second is direct interference, and the third is metasurface-induced interference.

Let

$$L_{x_0}(z) \triangleq \ell_{\mathrm{BM}}(\|z - x_0\|)\, \ell_{\mathrm{MU}}(\|z\|) \tag{6}$$

denote the two-hop attenuation through a metasurface at z. The geometry of the serving metasurface region then enters through

$$\begin{aligned} J_1(r) &\triangleq \int_{B(x_0, R_A)} \sqrt{L_{x_0}(z)}\, dz, \\ I_1(r) &\triangleq \int_{B(x_0, R_A)} L_{x_0}(z)\, dz. \end{aligned} \tag{7}$$

Conditioned on the serving distance $R_0 = r$, the useful signal power is approximated by $S \,|\, R_0 = r \sim \mathrm{Gamma}\big(k_S(r), \theta_S(r)\big)$, where $k_S(r)$ and $\theta_S(r)$ are obtained by moment matching. Similar Gamma-based approximations have been used in tractable analyses of multi-antenna and metasurface-assisted networks [21], [22]. A dedicated Monte Carlo validation is left to the full manuscript.

The link model is then carried to the network level through the coverage probability

$$p_c(\tau) = \int_0^\infty P(\tau \mid r)\, f_{R_0}(r)\, dr, \tag{8}$$

where $f_{R_0}(r) = 2\pi\lambda_{\mathrm{BS}}\, r\, e^{-\pi\lambda_{\mathrm{BS}} r^2}$ for $r \geq 0$. To evaluate $P(\tau \mid r)$, define

$$\mathcal{L}_{\sigma^2 + I_{\mathrm{agg}}}(s \mid r) \triangleq \mathbb{E}\Big[e^{-s(\sigma^2 + I_{\mathrm{agg}})} \,\Big|\, R_0 = r \Big].$$

If the derivative expansion is written with an integer-valued Gamma shape, let $\bar{k}_S(r)$ denote the integer shape used in that expansion, and let $\bar{\theta}_S(r)$ be the associated scale parameter chosen to preserve the conditional mean. The conditional success probability is obtained in tractable form as

$$P(\tau \mid r) = \sum_{m=0}^{\bar{k}_S(r)-1} \frac{(-1)^m}{m!} s^m \frac{d^m}{ds^m} \mathcal{L}_{\sigma^2 + I_{\mathrm{agg}}}(s \mid r) \Big|_{s = \tau/\bar{\theta}_S(r)}. \tag{9}$$

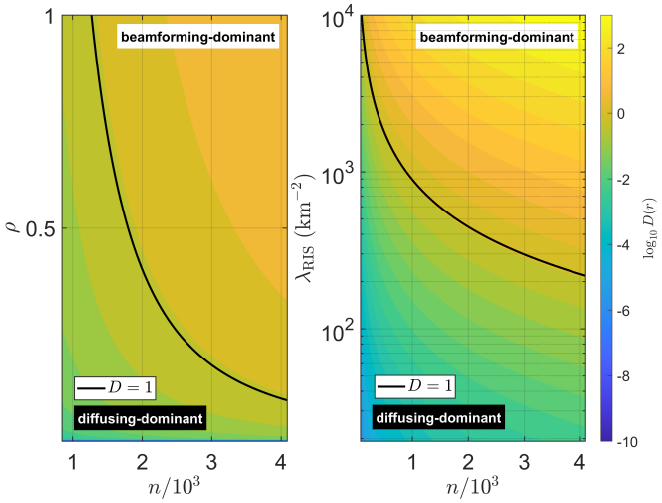

Fig. 2. Beamforming–diffuse regime map. Larger n (reflecting elements per surface), λ_M (surface density), or ρ (link-quality factor) favor beamforming. The black contour marks the approximate boundary.

Once $p_c(\tau)$ is available, the same framework yields spectral efficiency, average user rate, area spectral efficiency, area energy efficiency, and retransmission-sensitive performance.

A beamforming-dominance heuristic is

$$\lambda_{\mathrm{M}}^2 \Gamma^2 \zeta_b \eta\, \rho\, n^2 J_1^2(r) \gg \ell_{\mathrm{BU}}(r) + \lambda_{\mathrm{M}} \Gamma^2 \zeta_b \eta\, (1 - \rho)\, n\, I_1(r). \tag{10}$$

This inequality identifies the region in which the aligned reflected term dominates the direct link and the diffuse baseline. Outside that region, larger surfaces or denser RIS deployments do not improve network performance.

We also consider the area spectral efficiency, which measures how much data the network delivers per unit bandwidth and per unit area. Here $\beta \in [0, 1)$ denotes the resource overhead.

$$\mathrm{ASE}(\tau) = \lambda_{\mathrm{BS}}(1 - \beta)\, p_c(\tau)\, \log_2(1 + \tau). \tag{11}$$

III. Results

The results show that metasurfaces improve performance when the serving reflected link remains beamforming-dominant. In that regime, the reflected term is strong enough to increase the useful signal and reduce its variability. Unless stated otherwise, the figures are obtained by numerical evaluation of the analytical expressions under the 3GPP TR 38.901 UMi-LOS model at 3.5 GHz. When the operating point moves toward the diffuse regime, the average reflected power grows only linearly. Higher Doppler, larger control delay, or lower phase resolution reduce ρ and move the operating point toward the diffuse regime. Figure 2 summarizes this effect as a design map: larger n, larger ρ, or larger λ_{M} favor beamforming-dominant operation, while the black contour marks an approximate regime boundary.

Figure 3 shows the corresponding network-level effect. The hexagonal deployment curves lie above the Poisson curves as regular geometry suppresses the strongest irregular interferers.

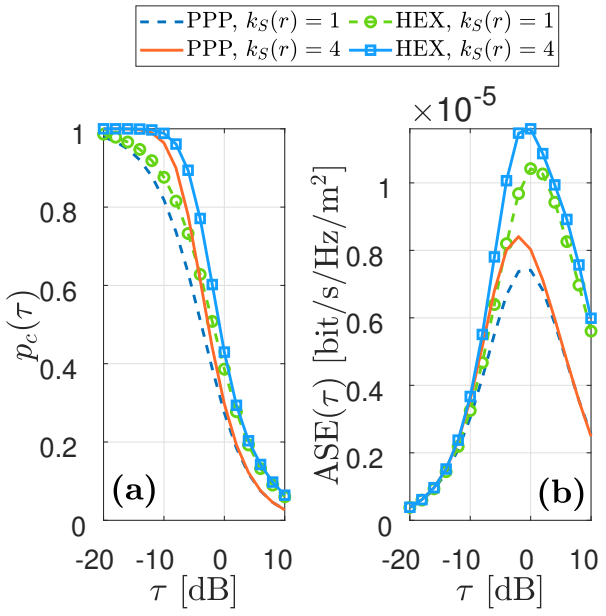

Fig. 3. Coverage probability $p_c(\tau)$ and area spectral efficiency $\mathrm{ASE}(\tau)$ for Poisson and density-matched hexagonal deployments, with SINR threshold τ and $k_S(r) \in \{1, 4\}$. Larger $k_S(r)$ indicates a more stable serving link.

$k_S(r)$ measures signal-power stability. Small $k_S(r)$ means strong fading. Large $k_S(r)$ means channel hardening. The gain is therefore not only a mean-power gain. It is also a stability induced by metasurfaces and captured by the Gamma model.

IV. Conclusion

This document describes a tractable analysis to identify when intelligent metasurfaces can improve cellular performance under realistic degradation. The main result is regime-dependent. Performance gains arise when the serving reflected term remains sufficiently coherent to strengthen and stabilize the useful signal without being offset by diffuse behavior and additional reflected interference. The analysis links this condition to coverage and area spectral efficiency. It therefore provides a first-order basis for judging when metasurface assistance is promising and when it is not. The contribution is deliberately limited in scope. Further work is needed on models for beam management, protocol signaling, insertion loss, calibration drift, grating lobes, near-field effects, interoperability, regulation, hardware validation, and techno-economic assessment. The present contribution focuses instead on the operating conditions that should inform those later stages.

Acknowledgment

The authors would like to thank Eitan Altman and Konstantin Avrachenkov from Inria, Lynda Zitoune from L2S, CentraleSupélec, and Software and Radio Architecture team at Orange S.A. for their valuable contributions to this work.

References

[1] M. D. Renzo, A. Zappone, M. Debbah, M.-S. Alouini, C. Yuen, J. de Rosny, and S. Tretyakov, "Smart radio environments empowered by reconfigurable intelligent surfaces: How it works, state of research, and the road ahead," *IEEE Journal on Selected Areas in Communications*, vol. 38, no. 11, pp. 2450–2525, 2020.

[2] E. Basar, M. D. Renzo, J. de Rosny, M. Debbah, M.-S. Alouini, and R. Zhang, "Wireless communications through reconfigurable intelligent surfaces," *IEEE Access*, vol. 7, pp. 116 753–116 773, 2019.

[3] Q. Wu and R. Zhang, "Towards smart and reconfigurable environment: Intelligent reflecting surface aided wireless network," *IEEE Communications Magazine*, vol. 58, no. 1, pp. 106–112, 2020.

[4] C. Pan, H. Ren, K. Wang, J. F. Kolb, M. Elkashlan, M. Chen, M. D. Renzo, Y. Hao, J. Wang, A. L. Swindlehurst, X. You, and L. Hanzo, "Reconfigurable intelligent surfaces for 6g systems: Principles, applications, and research directions," *IEEE Communications Magazine*, vol. 59, no. 6, pp. 14–20, 2021.

[5] Y. Zhu, G. Zheng, and K.-K. Wong, "Stochastic geometry analysis of large intelligent surface-assisted millimeter wave networks," *IEEE Journal on Selected Areas in Communications*, vol. 38, no. 8, pp. 1749–1762, 2020.

[6] T. Wang, G. Chen, M.-A. Badiu, and J. P. Coon, "Performance analysis of ris-assisted large-scale wireless networks using stochastic geometry," *IEEE Transactions on Wireless Communications*, vol. 22, no. 11, pp. 7438–7451, 2023.

[7] Y. Yuan, Y. Huang, X. Su, B. Duan, N. Hu, and M. D. Renzo, "Reconfigurable intelligent surface system level simulations for industry standards," *IEEE Communications Magazine*, vol. 63, no. 9, pp. 140–146, 2025.

[8] Q. Wu and R. Zhang, "Intelligent reflecting surface enhanced wireless network via joint active and passive beamforming," *IEEE Transactions on Wireless Communications*, vol. 18, no. 11, pp. 5394–5409, 2019.

[9] W. Tang, M. Z. Chen, X. Chen, J. Y. Dai, Y. Han, M. D. Renzo, Y. Zeng, S. Jin, Q. Cheng, and T. J. Cui, "Wireless communications with reconfigurable intelligent surface: Path loss modeling and experimental measurement," *IEEE Transactions on Wireless Communications*, vol. 20, no. 1, pp. 421–439, 2021.

[10] J. C. B. Garcia, A. Sibille, and M. Kamoun, "Reconfigurable intelligent surfaces: Bridging the gap between scattering and reflection," *IEEE Journal on Selected Areas in Communications*, vol. 38, no. 11, pp. 2538–2547, 2020.

[11] E. Björnson and L. Sanguinetti, "Power scaling laws and near-field behaviors of massive MIMO and intelligent reflecting surfaces," *IEEE Open Journal of the Communications Society*, vol. 1, pp. 1306–1324, 2020.

[12] A. Papazafeiropoulos, I. Krikidis, and P. Kourtessis, "Impact of channel aging on reconfigurable intelligent surface aided massive MIMO systems with statistical CSI," *IEEE Transactions on Vehicular Technology*, vol. 72, no. 1, pp. 654–669, 2023.

[13] A. Haskou and H. Khaleghi, "On the effect of RIS phase quantization on communications system performances," in *2023 IEEE 97th Vehicular Technology Conference (VTC2023-Spring)*, 2023, pp. 1–6.

[14] M. Åström, P. Gentner, O. Haliloglu, B. Makki, and O. Tageman, "Ris in cellular networks – challenges and issues," *CoRR*, vol. abs/2404.04753, 2024, submitted to IEEE Access.

[15] 3GPP, "Release 18," 3GPP Release Portal, 2024.

[16] ——, "Release 19," 3GPP Release Portal, 2025.

[17] ——, "Study on NR network-controlled repeaters," 3GPP, TR 38.867, 2022.

[18] ITU-R, "Framework and overall objectives of the future development of IMT for 2030 and beyond," ITU, Rec. M.2160-0, 2023.

[19] ITU-T SG5, "K.RIS_EMC: Electromagnetic compatibility requirements and measurement methods for RIS," Work Programme, Q4/5, 2025.

[20] J. G. Andrews, F. Baccelli, and R. K. Ganti, "A tractable approach to coverage and rate in cellular networks," *IEEE Transactions on Communications*, vol. 59, no. 11, pp. 3122–3134, 2011.

[21] X. Yu, C. Li, J. Zhang, M. Haenggi, and K. B. Letaief, "A unified framework for the tractable analysis of multi-antenna wireless networks," *IEEE Transactions on Wireless Communications*, vol. 17, no. 12, pp. 7965–7980, 2018.

[22] T. Wang, M.-A. Badiu, G. Chen, and J. P. Coon, "Outage probability analysis of star-ris assisted noma network with correlated channels," *IEEE Communications Letters*, vol. 26, no. 8, pp. 1774–1778, 2022.